

The association of hepatic fat percentage with selected anthropometric and biochemical parameters at 3-Tesla magnetic resonance imaging

A Al-Radaideh ^a, R Tayyem ^b, K Al-Fayomi^a, N Nimer^c, A Almomani^d, S Alhajjaj^e, L Agraib^b and N Hijjawi ^f

^aDepartment of Medical Imaging, Faculty of Applied Health Sciences, Hashemite University, Zarqa, Jordan; ^bDepartment of Nutrition and Food Technology, Faculty of Agriculture, University of Jordan, Amman, Jordan; ^cDepartment of Chemistry, College of Sciences and Health Professions, Cleveland State University, Cleveland, OH, USA; ^dDepartment of Radiology, King Hussien Medical Center, Jordanian Royal Medical Services, Amman, Jordan; ^eDepartment of Nutrition, King Hussien Medical Center, Jordanian Royal Medical Services, Amman, Jordan; ^fDepartment of Medical Laboratory Sciences, Faculty of Applied Health Sciences, Hashemite University, Zarqa, Jordan

ABSTRACT

Background and aim: This relatively comprehensive and multi-parametric study was conducted to investigate an association between hepatic fat percentage (HFP) values measured using high-field magnetic resonance imaging (MRI), anthropometric and biochemical measurements in healthy adults.

Methods: Abdominal MRI, anthropometric and biochemical measurements were determined in 156 healthy subjects. HFP values were derived from the MRI, whilst routine lipids, leptin, resistin, IL6 and adiponectin were measured by routine methods.

Results: Eighty per cent of the calculated HFP values were in the normal range of hepatic fat accumulation. Significant sex-adjusted correlations were found between HFP and waist circumference (WC) (measured by tape), BMI, leptin, resistin, WC (measured by MRI) and hip circumference (all $p < 0.001$) and triglycerides ($p = 0.01$). A significant inverse correlation was detected between HFP and adiponectin ($p < 0.001$).

Conclusions: A multi-parametric approach of MRI, biochemical and anthropometric measurements could be adopted to identify subjects at risk of developing non-alcoholic fatty liver disease.

ARTICLE HISTORY

Received 8 December 2018
Accepted 2 January 2019

KEYWORDS

Magnetic resonance imaging; hepatic fat percentage; anthropometry; lipid profile; adipokines; biochemistry

Introduction

Fat accumulation is one of the most common abnormalities of the liver detected on cross-sectional abdominal images [1]. This accumulation takes different patterns ranging from focal to diffuse fat accumulation which finally leads to a condition known as fatty liver [1]. The two most common types of fatty liver disease (FLD) are alcoholic and non-alcoholic fatty liver disease (NAFLD) [1]. Obesity, insulin resistant-diabetes mellitus (type 2-DM), hyperlipidemia, viral infection, overuse of certain drugs, dietary and nutritional abnormalities are among the well-known conditions which can enhance the development of NAFLD [1–3].

Measurement of plasma lipids (cholesterol, triglycerides, high-density lipoprotein (HDL), low-density lipoprotein (LDL)) and adipokine hormones (leptin and adiponectin) levels are important as defective lipid metabolism (disequilibrium in lipid homeostasis) can be an underlying cause for intrahepatic fat deposition [4]. Previous studies have showed that the visceral fat area and the body mass index (BMI) $> 158 \text{ cm}^2$ and 35 kg/m^2 , respectively, are strong predictors of NAFLD in 15–20% of obese patients [5,6].

The imaging approach of hepatic fat accumulation is preferred over the biopsy for its non-invasive nature,

qualitative and quantitative assessment of hepatic fat percentage (HFP) and concomitant screening for other liver abnormalities [2]. Magnetic resonance imaging (MRI) is an invaluable method for hepatic fat quantification, and different protocols have been used to assess hepatic fat accumulation [7–10]. However, gradient echo based-chemical shift imaging (GRE-CSI) with in-phase and out-of-phase acquisitions is the most widely used MRI technique for the assessment of fatty liver [1]. In GRE-CSI, the normal liver parenchyma has a similar signal intensity on both in and out of phase images, while fatty liver causes a signal loss on out of phase images [11]. While a triglyceride content above 5% is considered a cut-off point for diagnosing fatty liver according to the Non-alcoholic Steatohepatitis Clinical Research Network histologic scoring system [12], different HFP cut-off values (5.9% [13], 6% [14], 6.9% [15]), are suggested for diagnosing fatty liver on dual-echo and triple-echo MRI sequences.

This multi-parametric study was carried out to determine possible links between HFP values (measured using MRI) and selected anthropometric and biochemical measurements in a relatively comprehensive approach in a group of disease-free adults to help improve the level of understanding of the

associations of fatty liver with these factors. The latter would benefit those are at risk of developing NAFLD.

Materials and methods

The study was carried out in accordance with The Code of Ethics of the World Medical Association (Declaration of Helsinki). One hundred and fifty-six disease-free volunteers (83 males, 84 females; mean age 27.2 years; age range 18–51 years) met the inclusion criteria of this prospective cross-sectional study, that is, age > 18 years, disease-free, non-pregnant or lactating. Informed consent was obtained and MRI safety questionnaire was filled out by participants according to the approval of local research ethics committee (King Hussien Medical Center, Jordanian Royal Medical Services, Amman, Jordan). Demographic data collected included age, sex and tobacco use.

Anthropometric parameters, including weight, height, waist circumference (WC), hip circumference (HC) were obtained. Body weight and height measurements were carried out as indicated by Lee and Nieman (2013) [16]. BMI was calculated by dividing weight (in kilograms) by the square of height (in metres) and categorized as normal body weight (18.5–24.9 kg/m²), overweight (25.0–29.9 kg/m²) and obese (>30.0 kg/m²). WC was measured by tape (WC tape) at the narrowest level between the lowest rib and the iliac crest at the end of a normal expiration in standing position. WC was measured from the MR images (WC MRI) at a level just below the lower costal margin using image analysis software (SliceOmatic, Tomovision Inc., Montreal, Canada).

After 12-h overnight fasting, blood samples were collected separately in vacutainer plain tubes. Blood samples were allowed to clot at room temperature before being centrifuged at 4000 rpm for 5 min. The serum was frozen at –80°C until subsequent analysis. Adipokines (Adiponectin, Resistin and Leptin) and inflammatory cytokine interleukin 6 (IL-6) were measured by commercially available kits (RayBio® Human ELISA Kit, USA). Total cholesterol, LDL, HDL, and TG levels were measured using commercial kits (TECO Diagnostics, USA) by UV/Visible Spectrophotometer (Jenway 6305, USA).

MR images were acquired on a 3T Siemens Trio MR system (Siemens Healthcare, Erlangen, Germany), equipped with a 4-channel phased-array body coil. Consecutive (in-phase (IP₁), out-of-phase (OP), in-phase (IP₂)), breath hold, non-enhanced axial T1-weighted MR images were collected using a two-dimensional (2D) spoiled gradient-echo (GRE) MRI sequence. The second in-phase (IP₂) images were acquired to correct for the T2* decay as described by Guiu et al. [16]. which was, in part, derived from the original method that was proposed by Hussain et al [9]. The imaging parameters were as follows; repetition time (TR)/in-phase echo time (TE_{IP1})/out-of-phase echo time (TE_{OP})/in-phase echo time (TE_{IP2}) of

192/2.46/3.69/4.92 ms, 20° flip angle, 15 axial slices with slice thickness of 5 mm and 20% distance factor, 256 × 192 matrix size, 380 × 285 mm² field of view, number of signal averages of 1, and an acceleration factor of 2. All participants were instructed to hold their breath with full expiration while in a supine position. The axial slices were centered roughly at the level of the portal vein on coronal scout image. All abdominal MR images were checked for any artefact while the subject was still in the scanner. Fourteen participants were scanned twice due to some image artefacts (motion and/or phase error) and the images of their second scans were free of any obvious image artefacts.

The IP_(T2*corrected) and OP MR images were imported into JIM software (Jim version 7; Xinapse Systems, Northants, England). Signal intensities from regions of interest (ROIs) in the liver and spleen were recorded for IP_(T2*corrected) and OP images (Figure 1). For IP_(T2*corrected) images, three ROIs were obtained in the liver (two in the right lobe and one in the left lobe) in three sections. The three sections were selected to include levels above, at, and below the left portal vein. One more ROI was drawn in the spleen at the same three levels of liver's ROIs and used as an internal reference in order to decrease the differences due to scanner calibration. All 12 ROIs (nine in the liver and three in the spleen) had a similar area of 200 mm² and were copied to the OP images to make sure that all ROIs were drawn at similar positions between the two types of images. Each ROI included areas of parenchyma that did not contain vessels or image artefacts.

For IP_(T2*corrected) and OP images, the signal intensity of the liver was recorded as the mean of nine readings (SI_{liver}) from ROIs placed in the right and left lobes of the liver to account for signal heterogeneity. The signal intensity of the spleen was calculated as the mean of three readings (SI_{spleen}) from ROIs obtained in the spleen in three sections. As a result, each subject has two averaged signal intensities for the liver ROIs ($SI_{liver_ip_corrected}$, SI_{liver_op}) and two averaged signal intensities for the spleen ROIs ($SI_{spleen_ip_corrected}$, SI_{spleen_op}). Both, the ratio of the corrected averaged signal intensity (SIR) of the liver ROIs to that of the spleen ROIs on the T2*- corrected in-phase image ($(SIR_{liver-spleen})_{IP_corrected}$) and the ratio of the averaged signal intensity of the liver ROIs to that of the spleen ROIs on the out-of-phase image ($(SIR_{liver-spleen})_{OP}$) were used to calculate the HFP as follows [7]:

$$HFP = \left[\frac{(SIR_{liver-spleen})_{IP_corrected} - (SIR_{liver-spleen})_{OP}}{2(SIR_{liver-spleen})_{IP_corrected}} \right] \cdot 100$$

Data analysis was performed by SPSS 22.0 (SPSS Inc., Chicago, USA). HFP value of 5.9% was the cut-off point below which the hepatic fat accumulation

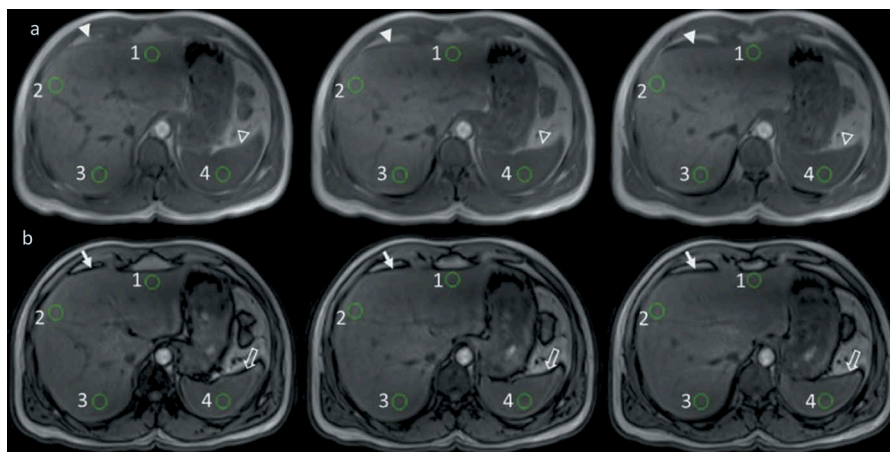


Figure 1. Non-enhanced, abdominal MRI images. (a) In-phase_{corrected} (first row), (b) out-of-phase (second row), MR images of the abdomen obtained in a 34-year-man at three levels; Above (first column), at (second column), and below (third column) the left portal vein. Fatty liver parenchyma shows a relative signal loss on the out-of-phase images. ROIs with similar area (200 mm²) were drawn in the liver and spleen at each level for the in-phase corrected and out-of-phase images. The signal intensity of the liver was recorded as the mean of nine readings from ROIs placed in the right (circles 2 and 3) and left (circle 1) lobes (three circles at each level) to account for signal heterogeneity. The signal intensity of the spleen was calculated as the mean of three readings from ROIs (circle 4) (one circle at each level). Each ROI included areas of parenchyma that did not contain vessels or image artefacts. Small arrows show areas of chemical shift-related signal void on the out-of-phase images (filled arrow: anterior border of the liver; hollow arrow: anterior border of the spleen). On the in-phase images, arrow heads (filled and hollow) point to the same anatomical borders, but do not exhibit any chemical shift-related signal void.

was considered normal [13]. Data were tested for normality and Pearson correlation coefficients were calculated by bivariate and multivariate regression analyses (after controlling for sex and age) to assess pairwise associations between MRI measured HFP, anthropometric, and biochemical parameters. For calculating the odd ratio (OR), its confidence interval (CI), and *p*-value for trend (*P-Trend*), logistic regression was used with age and sex adjustments.

Results

Eighty per cent (134/167) of the calculated HFP values from the IP_{corrected} and OP MR images were in the normal range of hepatic fat accumulation ($\leq 5.9\%$) with a median of 1.98 (IQR = 0.10–2.51). The remaining HFP values (33/167) were in the range of 6.4% to 32% with a median of 12.24 (IQR = 7.93–20.30). The descriptive characteristics of the study sample based on the HFP values are summarized in Table 1. High HFP values ($>5.9\%$) were seen in 19.8% (33/167) of subjects (mean/SD age 31.0 [8.9] years), with BMI (30.6 [4.5] kg/m²), WC-MRI (98.6 [9.6] cm) and HC (113.6 [2.88] cm). Ninety-four per cent (31/33) of the subjects with high HFP agreed to give a blood sample and had significantly higher serum levels of leptin, resistin, TG, cholesterol and LDL and lower serum levels of adiponectin than those with normal HFP values. While 69.7% of male participants had high HFP values, only 69.8% of female participants had normal HFP values.

The results of the correlation analysis (un-adjusted and adjusted for sex) between the HFP values with other factors including hormones, lipid profile, and anthropometric measures are summarized in Table 2. Significant sex-adjusted correlations were detected between HFP and WC tape, BMI, leptin, resistin, TG, WC-MRI, and HC. A significant inverse correlation was detected between HFP and adiponectin.

The sub-analysis of the correlation of HFP with anthropometric and biochemical measures based on sex (Table 3) showed that HFP correlates better in males than in females. For males, moderate to strong correlations were found between the HFP and BMI, leptin, resistin, IL-6, TG, LDL, WC-tape, WC-MRI and HC. While age and cholesterol level showed a weak correlation with HFP, adiponectin showed a moderate negative correlation with HFP. In females, weak to moderate correlations were found between HFP and BMI, WC-tape, WC-MRI, HC and weak negative correlation with adiponectin.

The results in Table 4 revealed that as the concentrations of leptin and IL-6 increase, the risk of having high HFP increases significantly at the 3rd and 4th quartiles. By contrast, adiponectin showed a significant negative link with fat in the liver at the 3rd and 4th quartiles. Triglycerides were the only lipid index where levels were significantly higher in the upper quartile. However, other lipid profile parameters showed a significant *P-Trend* when their

Table 1. Descriptive characteristics of the study subjects.

Parameter	HFP ($\leq 5.9\%$)	HFP ($> 5.9\%$)	P-Value
Age (years)	26.0 \pm 6.6	31.0 \pm 8.9	$P = 0.002$
Height (cm)	164.4 \pm 9.1	169.3 \pm 10.1	$P = 0.009$
Weight (kg)	70.3 \pm 12.5	87.5 \pm 14.3	$P = 0.001$
BMI (kg/m^2)	26.3 \pm 5.3	30.6 \pm 4.5	$P = 0.001$
WC (cm) by			
- Tape	87.5 \pm 10.6	101.3 \pm 10.6	$P = 0.001$
- MRI	84.3 \pm 12.5	98.6 \pm 9.6	$P = 0.001$
Leptin (ng/ml)	6.8 \pm 3.1	9.9 \pm 4.4	$P = 0.001$
Resistin (ng/ml)	8.0 \pm 3.9	10.9 \pm 4.4	$P = 0.001$
IL-6 (pg/ml)	9.0 \pm 4.6	10.6 \pm 5.1	$P = 0.081$
Adiponectin (pg/ml)	12.0 \pm 4.7	8.0 \pm 3.9	$P = 0.001$
Cholesterol (mmol/L)	4.0 \pm 0.8	4.4 \pm 1.1	$P = 0.022$
TG (mmol/L)	1.0 \pm 0.5	1.7 \pm 0.04	$P = 0.001$
HDL (mmol/L)	1.09 \pm 0.25	1.01 \pm 0.24	$P = 0.095$
LDL (mmol/L)	2.8 \pm 0.7	3.1 \pm 1.0	$P = 0.012$
Gender (n, %)			
Male	60 (44.8)	23 (69.7)	$P = 0.01$
Female	74 (55.2)	10 (30.3)	
BMI Categories (n, %)			
Normal	67 (54.0)	3 (9.4)	$P = 0.08$
Overweight	31 (25.0)	11 (34.4)	
Obese	26 (21.0)	18 (56.3)	
Smoking (n, %)			
Yes	32 (27.6)	9 (3.3)	$P = 0.634$
No	84 (72.4)	18 (66.7)	

Data presented as mean with SD. HFP-hepatic fat percentage; MRI-magnetic resonance imaging; BMI – body mass index; IL-6 – interleukin-6; TG – triglycerides; HDL – high-density lipoprotein cholesterol; LDL-low-density lipoprotein cholesterol; WC = waist circumference.

Table 2. Correlation coefficients (r) of HFP with anthropometric and biochemical parameters.

Parameter	HFP (r, P-value)	¥ HFP (r, P-value)
Age	(0.18, $P = 0.02$)	(-0.09, $P = 0.39$)
BMI (kg/m^2)	(0.40, $P < 0.001$)	(0.44, $P < 0.001$)
Leptin (ng/ml)	(0.43, $P < 0.001$)	(0.40, $P < 0.001$)
Resistin (ng/ml)	(0.36, $P < 0.001$)	(0.37, $P < 0.001$)
IL-6 (pg/ml)	(0.19, 0.02)	(0.19, $P = 0.08$)
Adiponectin (pg/ml)	(-0.37, $P < 0.001$)	(-0.36, $P < 0.001$)
Cholesterol (mmol/L)	(0.18, 0.02)	(0.06, $P = 0.56$)
TG (mmol/L)	(0.38, $P < 0.001$)	(0.28, $P = 0.01$)
HDL (mmol/L)	(-0.14, 0.09)	(-0.14, $P = 0.19$)
LDL (mmol/L)	(0.21, 0.01)	(0.04, $P = 0.68$)
WC (cm) by tape	(0.53, $P < 0.001$)	(0.49, $P < 0.001$)
WC (cm) by MRI	(0.46, $P < 0.001$)	(0.48, $P < 0.001$)
HC (cm)	(0.30, $P < 0.001$)	(0.41, $P < 0.001$)

Pearson's linear correlation coefficients are given. ¥ Adjusted for sex. Abbreviations as Table 1.

concentrations were tested for the association with HFP.

Discussion

In this study, in-phase and out-of-phase images were acquired using a triple-echo, T1-weighted spoiled gradient-echo pulse sequence and an ROI analysis was performed on the voxels in the liver relative to those in the spleen to estimate the hepatic fat accumulation. This MRI pulse sequence involved using a pair of in-phase echoes in addition to one out-of-phase echo. The pair of in-phase echoes were used to estimate the T2* time and correct for the signal decay between the first in-phase and out-of-phase echoes. Furthermore, the

Table 3. Correlation coefficients (r) of HFP with anthropometric and biochemical parameters based on sex.

Parameter	Male (N = 77) (r, P-value)	Female (N = 79) (r, P-value)
Age	0.29, $P = 0.01$	-0.11, $P = 0.33$
BMI (kg/m^2)	0.51, $P < 0.001$	0.32, $P < 0.001$
Leptin (ng/ml)	0.62, $P < 0.001$	0.17, $P = 0.14$
Resistin (ng/ml)	0.54, $P < 0.001$	0.19, $P = 0.10$
IL-6 (pg/ml)	0.35, $P < 0.001$	0.01, $P = 0.91$
Adiponectin (pg/ml)	-0.46, $P < 0.001$	-0.29, $P = 0.01$
Cholesterol (mmol/L)	0.29, $P = 0.01$	-0.04, $P = 0.72$
TG (mmol/L)	0.43, $P < 0.001$	0.19, $P = 0.10$
HDL (mmol/L)	-0.13, $P = 0.28$	-0.13, $P = 0.24$
LDL (mmol/L)	0.31, $P = 0.01$	0.01, $P = 0.94$
WC (cm) by tape	0.61, $P < 0.001$	0.41, $P < 0.001$
WC (cm) by MRI	0.58, $P < 0.001$	0.34, $P < 0.001$
HC (cm)	0.46, $P = 0.02$	0.24, $P = 0.04$

Abbreviations as Table 1.

relatively small flip angle and long TR that were used in the triple-echo MRI sequence reduced the effect of T1 relaxation. As a result, a more accurate and reliable hepatic fat quantification was possible.

Our cut-off HFP value (5.9%) was slightly different from those in related studies [13–15], in order to make a clear separation of the measured HFP values into two distinct groups (normal and high HFP values). Based on the HFP cut-off value, 80% of the calculated HFPs from the IP and OP MR images were in the normal range of hepatic fat accumulation. The results of the HFP analysis showed that 79.5% of the participants, who completed the three tests, had normal HFP values. Furthermore, 54% of the participants with normal HFP values had a normal BMI, while 56.3% of the participants with abnormal HFP values were obese. This was confirmed by the correlation analysis, which revealed a significant correlation between the HFP and BMI with and without gender adjustment. Furthermore, statistically significant moderate correlation was also found between HC, WC-MRI, WC-tape and HFP values. These findings indicate that the fatty liver incidence increases as the BMI increases. Waleed et al. carried out MR spectroscopy of the liver in 30 healthy controls and 15 patients with NAFLD and found a strong correlation between the mean hepatic fat contents and BMI, which ranged from 19.0 to 42.9 kg/m^2 [17]. Many other previous studies showed that the majority of patients with hepatic steatosis were found to be either overweight or obese [2,18,19] and the incidence of fatty liver is more frequent in obese than in lean subjects [20].

A statistically significant, but weak correlation was found between the HFP and subject's age with the abnormal HFP's subjects having significantly greater mean age than those with normal HFP values, indicating that the incidence of high HFP values increases with age. Furthermore, sex adjustment of the correlation coefficient of age with the HFP showed that the

Table 4. Odds ratios and 95% confidence intervals for biochemical parameters by HFP.

Parameter	HFP ($\leq 5.9\%$) N (%)	HFP ($> 5.9\%$) N (%)	Odds Ratio (95%CI)
Leptin (ng/ml)			
Q1	37 (29.6)	2 (6.5)	1 (-)
Q2	36 (28.8)	3 (9.7)	1.85 (0.28–12.03)
Q3	29 (23.2)	11 (35.5)	7.31 (1.44–37.20)
Q4	23 (18.4)	15 (48.4)	10.98 (2.14–56.19)
Resistin (ng/ml)			
Q1	38 (30.4)	2 (6.5)	1 (-)
Q2	34 (27.2)	4 (12.9)	1.30 (0.21–8.07)
Q3	27 (21.6)	12 (38.7)	5.73 (1.14–28.86)
Q4	26 (20.8)	13 (41.9)	7.45 (1.45–38.23)
IL-6 (pg/ml)			
Q1	33 (26.4)	6 (19.4)	1 (-)
Q2	32 (25.6)	7 (22.6)	1.27 (0.37–4.42)
Q3	31 (24.8)	8 (25.8)	1.49 (0.43–5.15)
Q4	29 (23.2)	10 (32.2)	1.76 (0.54–5.80)
Adiponectin (pg/ml)			
Q1	23 (18.4)	16 (51.6)	1 (-)
Q2	32 (25.6)	7 (22.6)	0.34 (0.11–1.02)
Q3	36 (28.8)	5 (16.1)	0.24 (0.07–0.82)
Q4	34 (27.2)	3 (9.7)	0.15 (0.04–0.64)
Cholesterol (mmol/L)			
Q1	34 (27.2)	6 (19.4)	1 (-)
Q2	32 (25.6)	6 (19.4)	0.88 (0.24–3.17)
Q3	33 (26.4)	7 (22.6)	1.21 (0.35–4.18)
Q4	26 (20.8)	12 (38.7)	1.51 (0.46–4.99)
Triglycerides (mmol/L)			
Q1	35 (28.0)	4 (12.9)	1 (-)
Q2	36 (28.8)	4 (12.9)	0.85 (0.19–3.74)
Q3	31 (24.8)	7 (22.6)	1.49 (0.38–5.85)
Q4	23 (18.4)	16 (51.6)	3.89 (1.07–14.15)
HDL (mmol/L)			
Q1	31 (24.8)	11 (35.5)	1 (-)
Q2	30 (24.0)	12 (38.7)	1.10 (0.39–3.07)
Q3	32 (25.6)	3 (9.7)	0.29 (0.07–3.07)
Q4	32 (25.6)	5 (16.1)	0.52 (0.07–1.19)
LDL (mmol/L)			
Q1	31 (24.8)	8 (25.8)	1 (-)
Q2	36 (28.8)	3 (9.7)	0.38 (0.09–1.62)
Q3	33 (26.4)	6 (19.4)	0.59 (0.17–2.02)
Q4	25 (20.0)	14 (45.2)	1.66 (0.56–4.91)

All OR trends $p < 0.001$. Q = quartile. HFP-hepatic fat percentage; CI—confidence interval. Odds ratio adjusted for age and sex.

age of males tends to show higher correlation values with the HFP than that of females. Although findings of some previous studies showed uncertainties regarding the influence of gender on NAFLD [21], our findings are in accordance with those from other studies [22–25]. In these studies, NAFLD was found to be more common in men than in women and this was attributed to different factors including the higher waist-to-hip circumference ratio in men compared to that in women and its effect on body weight [22], insulin resistance [26], sex hormones [23] and lifestyle [24]. The increase in weight during adult life could be attributed to age-related adiposity, hormonal changes, eating habits, metabolic rate, exercise and lifestyle changes [27,28].

A statistically significant weak to moderate positive correlation was detected between the HFP and TG, cholesterol and LDL levels when dividing the study sample into two groups according to their HFP values. In addition, cholesterol, LDL and TG were significantly

higher in subjects with abnormal HFP values than in those with normal HFP values indicating a strong connection between the hepatic fat accumulation and obesity-related biochemical factors. In addition, our results showed that a significant relationship between the 4th quartile of the triglyceride serum level and the risk of having high HFP. Overweight to obesity-related dyslipidemia and uncontrolled fatty acid release from adipose tissue, especially visceral adipose tissue, are manifested as an elevation of the serum levels of triglyceride and LDL and a reduction in the serum level of HDL. This could be attributed to the increase of endogenous hepatic fatty acids synthesis, the delivery of fatty acids to the liver, and the decrease in mitochondrial β -oxidation of fatty acids by the liver [31].

While elevated serum levels of leptin and resistin were significantly associated with increased risk of having high HFP values, high adiponectin serum levels showed a significant protective value from high HFP values. Hyperleptinemia and high resistin levels are linked to subcutaneous fat rather than visceral fat. However, hyperleptinemia may cause insulin resistance and influence visceral fat contents [32,33]. Adiponectin levels are negatively correlated with triglycerides and positively correlated with HDL cholesterol [34]. High adiponectin levels may stimulate fatty acid oxidation which induces activation of lipoprotein lipase and thereby enhancing the clearance of very low-density lipoprotein (VLDL) and reducing the plasma level of triglyceride in healthy adults with normal hepatic fat contents [35]. Several studies have examined links between NAFLD pathogenesis and adipokines such as leptin and adiponectin [4,32,36–38]. Leptin promotes inflammation and fibrogenesis [36], while adiponectin promotes insulin sensitivity and down-regulating the secretion of cytokines such as tumour necrosis factor alpha, IL-6, and IL-8 [4]. Both leptin and adiponectin stimulate AMP-dependent protein kinase in the liver and adipose tissues. This enzyme encourages glycolysis and fatty acid oxidation by activating peroxisome proliferator-activated receptor- α and preventing lipogenesis and cholesterol synthesis [37]. *De novo* hepatic lipogenesis significantly increases in NAFLD patients underlying the progression mechanism of hepatic steatosis [4,36]. The increase in leptin levels seems to contribute to insulin resistance and steatosis development, the latter results in a reduction in VLDL secretion and an increase in triglyceride accumulation in the liver indicating a disequilibrium in lipid homeostasis [4,36]. The rising prevalence of NAFLD might be due to the unhealthy lifestyle [39] and hypercaloric diet [40], which is strongly associated with obesity and long-term cardiovascular complications, an important global public health problem.

Although the MRI-HFP has been used and validated in many studies, this is the first to use the high-field (3T) MRI, anthropometric, and biochemical parameters to study the association of hepatic fat accumulation with different anthropometric and biochemical parameters in a group of disease-free adults. The strength of this study comes from the variety of biochemical and anthropometric parameters studied and linked to hepatic fat accumulation, which would improve the level of understanding of the associations of fatty liver with these factors. The latter would benefit those at risk of developing NAFLD. However, there are some limitations to our study. Liver histopathologic data were not obtained or used as a reference standard. In addition, our sample size was relatively small due to the difficulty of accessing the 3T MRI scanner. So, additional studies with a large number of participants and more concrete reference standards are required. A further limitation was the type of image analysis used, which was based on drawing a region of interests (ROIs) rather than whole liver analysis. This would affect the results of HFP as it depends on the position of the ROIs. However, the measurement of ROI in the whole liver can also result in an inaccurate fat percentage by including other anatomic structures such as vessels and bile ducts. Therefore, six ROIs were obtained from three levels in homogeneous parts of the liver parenchyma to avoid artefacts and vascular structures, as a representation of the whole liver along with three referenced ROIs in the spleen and at the same levels of the liver ROIs. Finally, the accuracy of the measured HFP values could also be affected by some confounding factors such as mineral deposition in the liver.

This work represents an advance in biomedical science because it shows the importance of studying the association of hepatic fat accumulation with different anthropometric and biochemical parameters, so providing a more reliable diagnosis of those at risk of NAFLD.

Summary Table

What is known about this subject:

- Liver biopsy is the current standard for diagnosing fatty liver, but it is an invasive procedure.
- MRI has been used as a non-invasive procedure in the diagnosis of fatty liver.
- Anthropometric and biochemical characteristics of patients with NAFLD are established.

What this paper adds:

- The combined approach of MRI, anthropometry and biochemistry can identify people who are at risk of developing NAFLD.
- Most anthropometric and biochemical parameters show a higher correlation with HFP in males than in females.

Acknowledgements

We would like to thank the Royal Medical Services for their great help and support and for allowing us to use their 3T MRI to scan our volunteers.

Disclosure statement

No potential conflict of interest was reported by the authors.

Funding

This research did not receive any specific grant from funding agencies in the public, commercial, or not-for-profit sectors.

ORCID

A Al-Radaideh  <http://orcid.org/0000-0002-6287-6716>

R Tayyem  <http://orcid.org/0000-0003-1640-0511>

N Hijjawi  <http://orcid.org/0000-0003-2489-5526>

References

- [1] Hamer OW, Aguirre DA, Casola G, et al. Fatty liver: imaging patterns and pitfalls. *Radiographics*. 2006; 26:1637–1653.
- [2] Ma X, Holalkere N-S, Kambadakone RA, et al. Imaging-based quantification of hepatic fat: methods and clinical applications. *Radiographics*. 2009;29:1253–1277.
- [3] Adams LA, Lymp JF, St Sauver J, et al. The natural history of nonalcoholic fatty liver disease: a population-based cohort study. *Gastroenterology*. 2005;129:113–121.
- [4] Sanyal AJ. Mechanisms of Disease: pathogenesis of nonalcoholic fatty liver disease. *Nat Clin Pract Gastroenterol Hepatol*. 2005;2:46–53.
- [5] Sobhonslidsuk A, Jongjirasiri S, Thakkinstian A, et al. Visceral fat and insulin resistance as predictors of non-alcoholic steatohepatitis. *World J Gastroenterol*. 2007;13:3614–3618.
- [6] Wanless IR, Lentz JS. Fatty liver hepatitis (steatohepatitis) and obesity: an autopsy study with analysis of risk factors. *Hepatology*. 1990;12:1106–1110.
- [7] Qayyum A, Goh JS, Kakar S, et al. Accuracy of liver fat quantification at MR imaging: comparison of out-of-phase gradient-echo and fat-saturated fast spin-echo techniques—initial experience. *Radiology*. 2005; 237:507–511.
- [8] Kim H, Taksali SE, Dufour S, et al. Comparative MR study of hepatic fat quantification using single-voxel proton spectroscopy, two-point dixon and three-point IDEAL. *Magn Reson Med*. 2008;59:521–527.
- [9] Hussain HK, Chenevert TL, Londy FJ, et al. Hepatic fat fraction: MR imaging for quantitative measurement and display—early experience. *Radiology*. 2005; 237:1048–1055.
- [10] Reeder SB, Hargreaves BA, Yu H, et al. Homodyne reconstruction and IDEAL water-fat decomposition. *Magn Reson Med*. 2005;54:586–593.
- [11] Pilleul F, Chave G, Dumortier J, et al. Fatty infiltration of the liver. Detection and grading using dual T1 gradient echo sequences on clinical MR system. *Gastroentérologie Clin Biol*. 2005;29:1143–1147.
- [12] Kleiner DE, Brunt EM, Van Natta M, et al. Design and validation of a histological scoring system for nonalcoholic fatty liver disease. *Hepatology*. 2005; 41:1313–1321.
- [13] Qayyum A, Nystrom M, Noworolski SM, et al. MRI steatosis grading: development and initial validation

- of a color mapping system. *AJR Am J Roentgenol.* **2012**;198:582–588.
- [14] Shin HJ, Kim HG, Kim M-J, et al. Normal range of hepatic fat fraction on dual- and triple-echo fat quantification MR in children. *PLoS One.* **2015**;10:e0117480.
- [15] Leitão HS, Paulino C, Rodrigues D, et al. MR fat fraction mapping: a simple biomarker for liver steatosis quantification in nonalcoholic fatty liver disease patients. *Acad Radiol.* **2013**;20:957–961.
- [16] Guiu B, Petit J-M, Loffroy R, et al. Quantification of liver fat content: comparison of triple-echo chemical shift gradient-echo imaging and in vivo proton MR spectroscopy. *Radiology.* **2009**;250:95–102.
- [17] Ismail W, Ismail WAF, Abdelhai AR, et al. Evaluation of liver fat content with magnetic resonance spectroscopy in overweight subjects as an early detector of fatty liver disease and correlation with liver biopsy. *J Gastroenterol Hepatol Res.* **2014**;3:1150–1155.
- [18] López-Velázquez JA, Silva-Vidal KV, Ponciano-Rodríguez G, et al. The prevalence of nonalcoholic fatty liver disease in the Americas. *Ann Hepatol.* **2014**;13:166–178.
- [19] Vernon G, Baranova A, Younossi ZM. Systematic review: the epidemiology and natural history of non-alcoholic fatty liver disease and non-alcoholic steatohepatitis in adults. *Aliment Pharmacol Ther.* **2011**;34:274–285.
- [20] Thomas EL, Hamilton G, Patel N, et al. Hepatic triglyceride content and its relation to body adiposity: a magnetic resonance imaging and proton magnetic resonance spectroscopy study. *Gut.* **2005**;54:122–127.
- [21] Pan -J-J, Fallon MB. Gender and racial differences in nonalcoholic fatty liver disease. *World J Hepatol.* **2014**;6:274–283.
- [22] Clark JM, Brancati FL, Diehl AM. The prevalence and etiology of elevated aminotransferase levels in the United States. *Am J Gastroenterol.* **2003**;98:960–967.
- [23] Denzer C, Thiere D, Mucbe R, et al. Gender-specific prevalences of fatty liver in obese children and adolescents: roles of body fat distribution, sex steroids, and insulin resistance. *J Clin Endocrinol Metab.* **2009**;94:3872–3881.
- [24] Williams CD, Stengel J, Asike MI, et al. Prevalence of nonalcoholic fatty liver disease and nonalcoholic steatohepatitis among a largely middle-aged population utilizing ultrasound and liver biopsy: a prospective study. *Gastroenterology.* **2011**;140:124–131.
- [25] Weston SR, Leyden W, Murphy R, et al. Racial and ethnic distribution of nonalcoholic fatty liver in persons with newly diagnosed chronic liver disease. *Hepatology.* **2005**;41:372–379.
- [26] Ruhl CE, Everhart JE. Determinants of the association of overweight with elevated serum alanine aminotransferase activity in the United States. *Gastroenterology.* **2003**;124:71–79.
- [27] Vincent HK, Raiser SN, Vincent KR. The aging musculoskeletal system and obesity-related considerations with exercise. *Ageing Res Rev.* **2012**;11:361–373.
- [28] Green CJ, Hodson L. The influence of dietary fat on liver fat accumulation. *Nutrients.* **2014**;6:5018–5033.
- [29] Ferramosca A, Zara V. Modulation of hepatic steatosis by dietary fatty acids. *World J Gastroenterol.* **2014**;20:1746–1755.
- [30] Giby VG, Ajith TA. Role of adipokines and peroxisome proliferator-activated receptors in nonalcoholic fatty liver disease. *World J Hepatol.* **2014**;6:570–579.
- [31] Kazmi A, Sattar A, Hashim R, et al. Serum leptin values in the healthy obese and non-obese subjects of Rawalpindi. *J Pak Med Assoc.* **2013**;63:245–248.
- [32] Schäffler A, Schölmerich J, Büchler C. Mechanisms of disease: adipocytokines and visceral adipose tissue—emerging role in nonalcoholic fatty liver disease. *Nat Clin Pract Gastroenterol Hepatol.* **2005**;2:273–280.
- [33] Berneis KK, Krauss RM. Metabolic origins and clinical significance of LDL heterogeneity. *J Lipid Res.* **2002**;43:1363–1379.
- [34] Donnelly KL, Smith CI, Schwarzenberg SJ, et al. Sources of fatty acids stored in liver and secreted via lipoproteins in patients with nonalcoholic fatty liver disease. *J Clin Invest.* **2005**;115:1343–1351.
- [35] Stojšavljević S, Gomerčić PM, Virović JL, et al. Adipokines and proinflammatory cytokines, the key mediators in the pathogenesis of nonalcoholic fatty liver disease. *World J Gastroenterol.* **2014**;20:18070–18091.
- [36] Hassan K. Nonalcoholic fatty liver disease: A comprehensive review of a growing epidemic. *World J Gastroenterol.* **2014**;20:12082–12101.
- [37] Nseir W, Hellou E, Assy N. Role of diet and lifestyle changes in nonalcoholic fatty liver disease. *World J Gastroenterol.* **2014**;20:9338–9344.
- [38] Jump DB, Depner CM, Tripathy S, et al. Impact of dietary fat on the development of non-alcoholic fatty liver disease in *Ldlr*^{-/-} mice. *Proc Nutr Soc.* **2015**;75:1–9.